

Gaia duplicity detection: photocentric binaries

Frédéric Arenou & Carme Jordi

GAIA-FA-02

Rev 1.5, May 10, 2001

Abstract

Thanks to its broad band photometric measurements, Gaia may be also able to detect binaries separated by a few milliarcseconds, with magnitude differences between 1 and 5 mag. Together with the geometry of the system, the magnitude and colour of each component will be recovered approximately.

1 Introduction

The “red book” assumes that binaries observed by Gaia may be resolved for a separation larger than 20 mas. The information from the broad band photometers has however not been taken into account.

Just in order to get an order of magnitude of what can be done with the broad bands, let us take an example, with simplifications (in the next section, more realistic simulations are presented).

Consider for instance a 12^m G0 with an M0 companion. The magnitude difference is 4.4 in a V band, but 3 mag in a I band. Thus, the difference of position of the photocentre between these two bands is $s[(1 + 10^{0.4*4.4})^{-1} - (1 + 10^{0.4*3})^{-1}] = 0.042s$ where s is the separation ρ between components projected onto the great circle. When this positional difference is larger (e.g. at 3σ) than the positional precision, then there is an indication of duplicity.

The positional precision in the broad bands may be evaluated roughly the following way: due to the 1×8 BBP samples in Astro 1, just like what is done in the astrometric field, the final astrometric precision in one of the BBP band is about $\sqrt{32} \times$ the precision in the G band (16 CCD in the preceding and following FOV) that is $\sqrt{32} \times 0.004$ mas (neglecting here the smaller flux in the BBP).

Concerning our example, a separation $\rho = 3 \sqrt{2} \sqrt{32} 0.004 / 0.042 = 2.3$ mas can thus be detected at 3σ . Just like Hipparcos which introduced the VIM or acceleration solutions, Gaia will introduce a new category which may be called photocentric binaries or *color-induced displacements* in the terminology of [Wielen 1997]. This suggestion had also been formulated by [Tokovinin 1999].

2 Simulations

We simulated how the astrometric and photometric measurements of the components can be recovered. For a wide range in period, distance, and magnitude difference between components, and a primary of absolute magnitude $V = 5$, the position and magnitude of the photocentre has been computed in the G band and the 4 broad bands for each transit. Then a least-square program tries to recover the photometric information about components (V magnitude and $V - I$ colour) and the geometry of the system from the average ≈ 67 transits.

For a given period, distance and magnitude difference, the apparent V magnitudes, ($V - I$) colors, masses of each components have been simulated using a classical main-sequence relation, with no intrinsic dispersion.

Our simulations have been done in terms of V and $V - I$ although using G and e.g. $45B - 82B$ for magnitude and colour could have given results more adapted to the Gaia case. However V and $V - I$ are more widely known, and provide results less dependent on the final photometric system which will be chosen for Gaia. The transformation from V and $V - I$ to the G band has been computed according to the red book (Eq. 29, p. 239). Concerning the transformation to the 4 broad bands, the following relations

$$\left\{ \begin{array}{l} V - 33B = +0.165 - 3.623(V - I) + 5.908(V - I)^2 - 6.167(V - I)^3 + 1.837(V - I)^4 \\ V - 45B = +0.046 - 0.854(V - I) - 0.188(V - I)^2 + 0.125(V - I)^3 \\ V - 63B = -0.003 + 0.303(V - I) + 0.195(V - I)^2 - 0.100(V - I)^3 \\ V - 82B = +0.000 + 0.999(V - I) \end{array} \right\} \quad (1)$$

have been tested, but better results have been obtained using

$$\left\{ \begin{array}{l} G - 33B = +0.110 - 3.867(V - I) + 5.069(V - I)^2 + 5.316(V - I)^3 - 19.073(V - I)^4 + 13.436(V - I)^5 \\ \quad - 2.883(V - I)^6 \\ G - 45B = -0.011 - 0.059(V - I) - 1.629(V - I)^2 + 1.290(V - I)^3 - 0.570(V - I)^4 + 0.114(V - I)^5 \\ G - 63B = -0.035 + 1.052(V - I) - 1.712(V - I)^2 + 1.983(V - I)^3 - 1.094(V - I)^4 + 0.205(V - I)^5 \\ G - 82B = -0.047 + 1.835(V - I) - 1.583(V - I)^2 + 1.018(V - I)^3 - 0.243(V - I)^4 \end{array} \right\} \quad (2)$$

with respective magnitude zero-points indicated in Table 1.

Table 1: Zero-point magnitude (meaning here $1e^-$ for the 0.86s observation) and extinction ratio.

band b	zero-pt	A_b/A_V
G	26.320	0.85
$33B$	23.614	1.65
$45B$	25.403	1.27
$63B$	25.120	0.86
$82B$	23.729	0.60

Our simulations are limited to a ≈ 5 mag magnitude difference between components since the above equations are valid up to about absolute magnitude $G = 10$ and the primary is of absolute magnitude 5.

Instead of using the true scanning law, random satellite orientations have been generated in order to compute the position of the photocentre at each of the 67 observation epochs. For “small” periods, the orbit itself should be used. This aspect is not studied here: it has been assumed that the orbit of the photocenter is of null eccentricity and inclination and that the orbital parameters have been recovered through the G band astrometric study, so that at each observation epoch the position angle would be known. It may happen (when the mass ratio is equal to the flux ratio in the G band) that the orbit remains undetected: once again, thanks to the broad bands, the motion may be detected in some cases at a different wavelength (and also by the RVS instrument). In practice, a simultaneous resolution of the orbital elements, flux ratio in each band and astrometric parameters of the barycenter should be implemented. This could be the subject of another study.

On a single CCD transit, the precision on magnitudes in a given band b has been calibrated using the curves in the red book (Fig. 8.8, p. 276) with

$$\log \sigma_b = 1.7054 - 1.4187L + 0.1736L^2 - 0.0108L^3 \quad (3)$$

noting L the log of the flux in that band, limited to the CCD saturation ($500\,000 e^-$). We did not take into account any limiting systematic (calibration) error on photometry partly because we assume that it plays a minor role in the “differential measurements” between bands at a given epoch, and also because it will be small compared to the final random errors on the extracted magnitudes of each component.

The relations (2) are not well adapted to reddened data. For the simulations, an extinction law ($A_V = 0.5$ mag/kpc) has been however added to the photometry in each band using the ratio indicated in Table 1. After the computation of the formal error on photometry, the reddening has been subtracted since we assume that it may be computed in the real Gaia case using the 11 medium bands.

The along-scan epoch astrometric precision σ_x in a given band has been computed using the relation given for the parallax precision (red book, Eq. 81, p. 267), adapting it to the actual flux received in this band, and multiplying it by $\sqrt{67 \times 32}$. This could be conservative, since what is needed here are the differential positions between bands, and part of the instrument and astrometric parameters, taken into account in the red book, removed degrees of freedom. Although not really useful, the across-scan position was also computed, and its precision was assumed to be $\sigma_y = 3 \times 8 \times \sigma_x$.

The astrometric and photometric epoch precisions have been assumed to be $\sqrt{32}$ more precise in the G band than in the broad bands. Finally, the “observed” photometric and astrometric data of each epoch photocenter magnitude and position have been generated with a Gaussian noise using the above quoted precisions.

3 Detection limits of photocentric displacements

The least-square detection program implements the same transformation equations (2) from V and $V - I$ to G and the 4 BBP bands, and tries to recover $\rho, \theta, x_A, y_A, V_A, (V - I)_A, V_B, (V - I)_B$, where (x_A, y_A) is the position of the primary and (ρ, θ) the respective separation and position angle of the secondary.

The tested periods are (0.1, 0.5, 1, 5, 10, 50, 100, 500, 1000) years, the tested ΔV magnitude differences are (0.1, 1, 2, 3, 4, 5, 6) mag for distances between 200 and 3600 pc.

Almost no result is obtained for $\Delta V = 0.1$ due to the small colour difference between components. It appears also that in some of the simulations, no sensible solution could be found. This is mostly due to the non-linearity of the least-square program, but also due to the fact that the color transformations equations (2) could diverge when the least-square program tries to use a large $V - I$. But this could be accounted for in the least-square model.

Only the solutions for which a detection ($\rho > 3\sigma_\rho$) is achieved have been plotted Fig. 1. While each line depends on the period (i.e. separation), the points in each line are those obtained at various distances

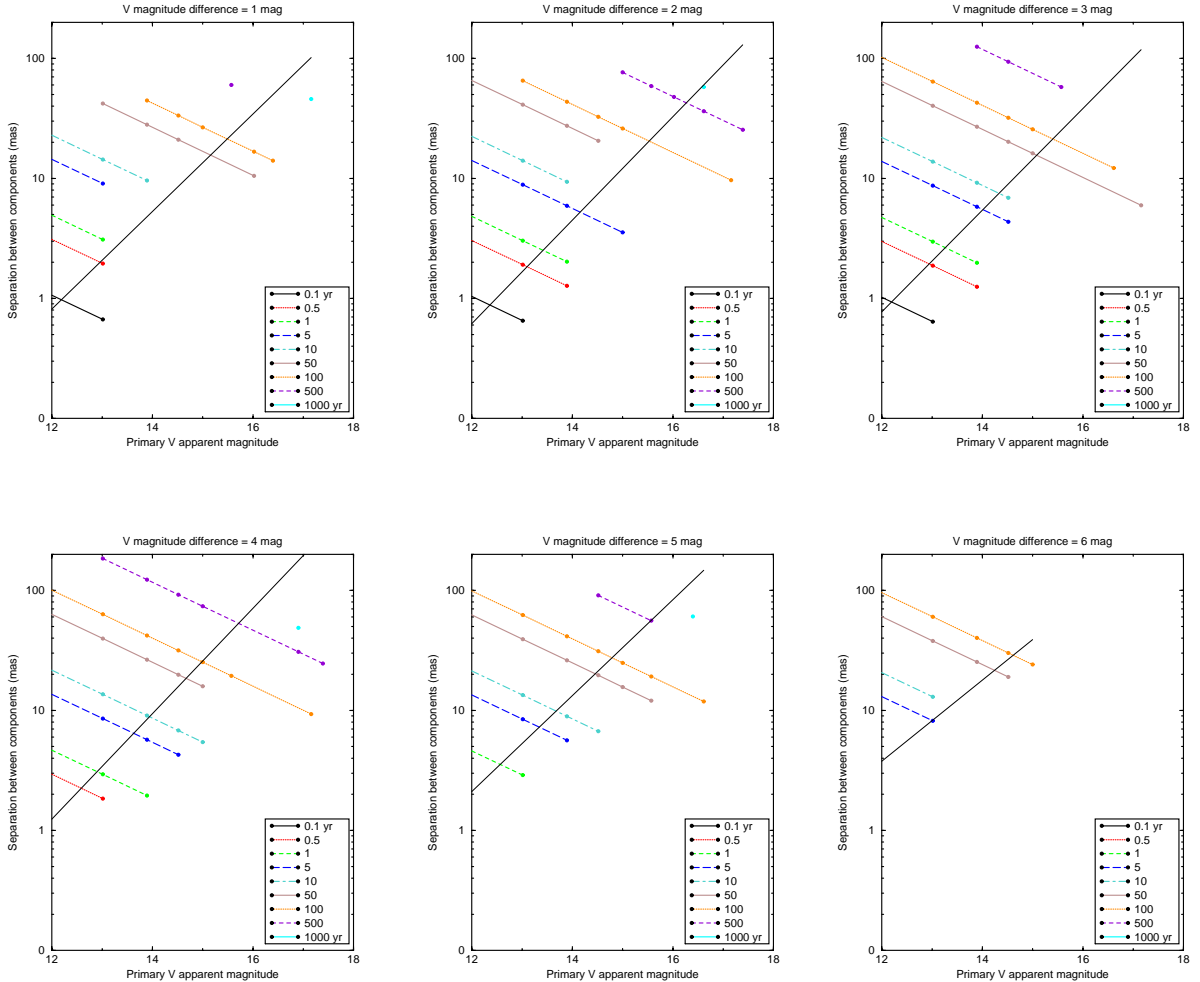


Figure 1: Detections ($\text{SNR}_\rho > 3$) for ΔV between 1 and 6 mag for different orbital periods (ρ versus V_A). The transverse line is the average 3σ value obtained with Eq. 4.

(i.e. apparent magnitude, since the absolute magnitude is fixed here). A sub-milliarcsecond precision may be achieved for the brighter stars with a magnitude difference in the range 1-3 mag.

The shape of achievable separation, Fig. 1, is not unexpected. In the range of magnitudes we used (i.e. with no saturation and a small effect of RON noise), the photon noise plays the major role (flux at the power $-1/2$), and thus the log of the astrometric precision is approximately linear with the magnitude. Since we used a $\rho > 3\sigma_\rho$ detection level, we then expect the log of the separation to be above a given line as a function of magnitude.

For simulation purposes, it may however be more convenient to have an estimate of the separation precision as a function of the astrometric precision of the binary σ_π . Using all results from the simulations, the following empirical fit, where ρ , σ_π and σ_ρ are in mas,

$$\sigma_\rho \approx \sqrt{\rho} \frac{10^{1.65+0.22\Delta V}}{\Delta V} \sigma_\pi \quad (4)$$

although with a 60% dispersion, provides a rough estimate of the achievable precision on the separation.

It must be pointed out that the assumed astrometric precision is conservative, that we did not make use of the following field of view, nor of the 11 photometric bands. The possibility to implement 5 broad bands instead of 4 would not have a major impact on the above result, since the detection efficiency is probably due mainly to the photocenter differential position between the extreme (33B and 82B) bands.

Some magnitudes and colours of the secondaries, output from the least-square solution may be found Fig. 2; they are clustered around the true input values ($V = 6, 7, 8, 9, 10, 11$). This can't be used for a precise mass-luminosity relation, but this allows to classify approximately the faint secondaries: a secondary with magnitude $V = 20$ gets a photometric precision ≈ 0.2 on colour and ≈ 0.3 on V magnitude.

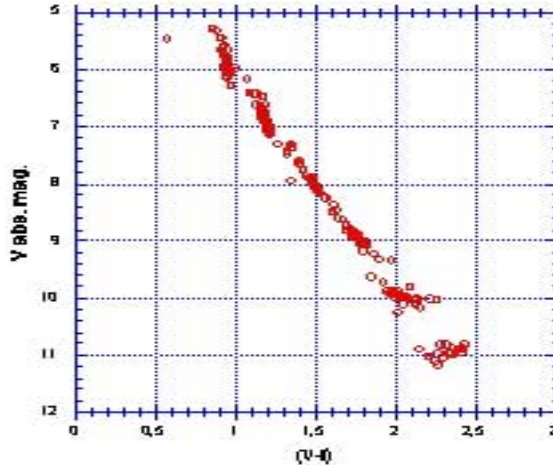


Figure 2: H-R diagram of detected secondaries.

4 Conclusion

The first sentence concerning the census of binaries in the (white) red book mentioned that “*Gaia will not resolve binaries with separations below ≈ 20 mas which today is routinely achieved from the ground by speckle interferometry*”. In fact, Gaia may possibly compete with long baseline optical and infrared interferometry, although for fainter and much more numerous binaries: through the photocentric effect, it happens that the brighter binaries with a few milliarcsecond separation may be detected, for the mass ratio range $\approx 0.5 - 0.9$ (for main-sequence stars), and giving an estimate of the magnitude and colour of each component.

Because Gaia is a complete space-based observatory, it will be able to detect the following various categories of binaries:

- resolved binaries (above ≈ 20 mas)
- astrometric binaries (stochastic or acceleration)
- spectroscopic binaries
- photocentric binaries
- variable-induced movers
- eclipsing binaries
- light-time orbits (see SAG-FA-001)

In the (distance, period, magnitude-difference) space, these different methods overlap, and in general masses can be obtained only when combining two different methods. From Fig. 1, photocentric binaries which are detected without being resolved overlap with the astrometric binaries, while, depending on the period, the RVS instrument will or will not detect the duplicity. For a short period, and a small magnitude difference, the star will probably also be SB2, and individual masses and fluxes will be recovered. The overlapping of these methods also allows a lower detection threshold. This issue remains to be studied.

References

- [Tokovinin 1999] Tokovinin, 1999, Atelier Gaia, “l’astrométrie pour l’astrophysique et l’astrodynamique”, Grasse, 17-18 juin 1999
- [Wielen 1997] Wielen, 1997, A&A 325, 367